Published in final edited form as:
Cancer Lett. 2012 September 1; 322(1): 58–69. doi:10.1016/j.canlet.2012.02.005.

K-*Ras* mutation-mediated IGF-1-induced feedback ERK activation contributes to the rapalog resistance in pancreatic ductal adenocarcinomas

Feng Wei, **Yan Liu**, **Anita C. Bellail**, **Jeffrey J. Olson**, **Shi-Yong Sun**, **Guoyue Lu**, **Lijuan Ding**, **Changji Yuan**, **Guangyi Wang**, and **Chunhai Hao**

Abstract

Mammalian target of rapamycin complex 1 (mTORC1) is frequently activated in human cancers; however, clinical trials of rapalog (the mTORC1 inhibitors) have shown that pancreatic ductal adenocarcinomas (PDACs) resist to the treatment. Rapalog treatment activated the extracellular signal-regulated kinase (ERK) pathway in K-*Ras* mt PDAC cells. K-*Ras* knockdown abolished the insulin-like growth factor-1 (IGF-1)-induced ERK pathway in the K-*Ras* mt PDAC cells and enhanced the therapeutic efficacy of everolimus in treating K-*Ras* mt PDAC cells-derived mouse xenografts. The results indicate that targeting of K-*Ras* mutation may lead to the development of therapies that overcome rapalog resistance in PDAC.

Keywords

K-*Ras*; mTORC1; rapalog; ERK; pancreatic cancer

1. Introduction

Mammalian target of rapamycin (mTOR) of the phosphatidylinositol 3-kinase (PI3K)-related protein kinase family [1] has recently emerged as a cancer therapeutic target [2]. mTOR exists in two distinct functional complexes: mTOR complex 1 (mTORC1) and mTOR complex 2 (mTORC2). mTORC1 controls protein translation through phosphorylation and activation of its substrates, p70S6 ribosomal kinase (p70S6K) and eukaryotic translational initiation factor 4E (eIF4E) binding protein (4E-BP1) [3]. Once phosphorylated, 4E-BP1 dissociates from eIF4E whereas p70S6K phosphorylates ribosomal protein S6, thus promoting mRNA translation [3]. The defining component of mTORC1 is the regulatory-associated protein of mTOR (RAPTOR) that regulates mTORC1 assembly and recruitment of its kinase substrates [4]. Rapamycin is a macrolide antibiotic that can remove RAPTOR from mTORC1 and thus inhibits mTORC1 phosphorylation of its substrates [5]. This mTORC1 pathway is activated in many cancers and drives cancer progression [6]. The rapamycin analogs everolimus (RAD001), temsirolimus (CCI-779) and ridaforolimus (AP23573) have therefore been developed as cancer therapeutic agents [7; 8]. In phase III trials, single-agent everolimus and temsirolimus prolonged overall survival of patients with advanced renal cell carcinoma [9; 10], mantle cell lymphoma [11] and

Conflicts of Interest The authors declare no conflicts of interest.

pancreatic neuroendocrine tumor [12]. In phase II trials, however, the single-agent therapies have had limited clinical activity against glioblastomas [13], advanced melanomas [14], breast cancers [15; 16] and pancreatic ductal adenocarcinomas (PDAC) [17; 18]. The molecular basis of rapalog resistance in these cancers is currently under intensive investigation.

mTORC1 acts as a central integrator for upstream inputs from growth factors, nutrients and stress [19]. Growth factors such as insulin and insulin-like growth factor-1 (IGF-1) can activate mTORC1 through their cognate receptor tyrosine kinase (RTK)-mediated phosphorylation and activation of PI3K and Akt [19]. Akt phosphorylates its substrates tuberous sclerosis 2 (TSC2) and proline-rich Akt substrate 40 kDa (PRAS40), thus releasing their inhibition of mTORC1 [20; 21]. The growth factors can also signal mTORC1 through Ras-extracellular signal-regulated kinase (ERK) signaling pathway [22]. The Ras-ERK pathway consists of Ras GTPase and the protein kinases Raf, mitogen-activated protein kinase (MAPK)/ERK kinase (MEK) and ERK. RTK-mediated activation of the Ras GTPase leads to the activation of these kinases through phosphorylation loops: Raf activates MEK, MEK activates ERK and ERK activates p90 ribosomal S6 kinase (RSK) [22]. Both ERK and RSK phosphorylate the mTORC1 inhibitor TSC2 [23; 24] and ERK phosphorylates RAPTOR [25], thus promoting the activation of mTORC1. This growth factor-mTORC1 pathway is regulated through two negative feedback loops: mTORC1-S6K-mediated phosphorylation and degradation of insulin receptor substrate (IRS) [26; 27] and mTORC1-mediated phosphorylation of growth factor receptor-bound protein 10 (Grb10) [28]. Through these negative feedback loops, rapalogs inhibit mTORC1 and activate PI3K [18; 29; 30; 31] and ERK in cancers [32], resulting in cancer resistance to the treatment.

Ras GTPases are coded by the human H-*Ras*, K-*Ras* and N-*Ras* genes. K-*Ras*, but not H-*Ras* or N-*Ras*, is frequently mutated in nearly 95% human PDACs [33]. Mutant (mt) K-Ras proteins exhibit constitutive GTPase activity [34] and thus contribute to the development and progression of PDAC [35]. Here, we show that K-*Ras* mutations play a critical role in the rapalog resistance in PDAC. K-*Ras* mutations contribute to the rapalog-induced feedback activation of IGF-1-Ras-Raf-ERK pathway and inhibition of the mt K-Ras abolishes the feedback ERK signal, reduces the rapalog resistance and thus enhance inhibitory effect of rapalog on the growth of K-Ras mt PDAC cells-derived mouse xenografts.

2. Materials and Methods

2.1. Human pancreatic carcinoma cell lines, tissues and normal pancreatic tissues

Human PDAC cell lines, BxPC-3, Capan-2, Hs 766T, and PANC-1 were obtained from the American Type Culture Collection (Rockville, MD). BxPC-3 was grown in RPMI-1640 medium (Invitrogen, Carlsbad, CA); Capan-2 in McCoy 5α medium (Invitrogen); and Hs 766T and PANC-1 were in DMEM (Invitrogen) supplemented with 10% FBS (Invitrogen). Human PDAC and normal pancreatic tissue samples were collected in accordance with protocols approved by the Institutional Review Board of the First Hospital of Jilin University. These tissues were surgically removed from patients diagnosed with PDAC, snap-frozen and stored at − 80°C.

2.2. Reagents and antibodies

Everolimus (RAD001) and sorafenib from LC Laboratories (Woburn, MA) were dissolved in dimethyl sulfoxide at a concentration of 20 mM and stored in aliquots at −80°C. NVP-AEW541 (hydrochloride) was purchased from Cayman Chemical (Ann Arbor, MI) and dissolved in PBS at a concentration of 10mM and stored in aliquots at −80°C. Recombinant

human IGF-1 (rhIGF-1) was purchased from R&D systems (Minneapolis, MN). From Cell Signaling Technology (Beverly, MA) were the antibodies to 4E-BP1, phospho-4EBP1 (p-4E-BP1; Ser37/46), Akt, p-Akt (Ser473), p-ERK1/2 (Thr202/Tyr204), green fluorescent protein (GFP), p-MEK1/2 (Ser217/221), mTOR, p-mTOR (Ser2448), p70S6K, p-p70S6K (Thr389), ribosomal protein S6 (S6), p-S6 (Ser235/236), and p-RSK (Ser380). Actin and K-Ras antibody were purchased from Santa Cruz (Santa Cruz, CA). Horseradish peroxidase (HRP)-conjugated goat anti-mouse and goat anti-rabbit antibodies were from Jackson IR Laboratories (West Grove, USA).

2.3. PCR and restriction fragment length polymorphism (RFLP) analysis

Total RNA was extracted from snap-frozen tissues and cell cultures by using Trizol (Invitrogen) according to the manufacturer's protocols. cDNA was synthesized using 2μg of total RNA with SuperScript II First-Strand Synthesis using oligo (dT) primer System following the manufacturer's protocols (Invitrogen). Aliquots of the reaction mixture were used for the subsequent PCR amplification. The primer sequences for KRAS amplification were: sense: 5'-GACTGAATATAAACTTGTGGTAGTTGGACCT-3' and antisense: 5'-TCCTCTTGACCTGCTGTGTCG-3'. The sense primer was designed to introduce a base substitution that created a BstNI recognition site for the WT codon 12 (GGT), but not for codon 12 with the KRAS mutation. PCR conditions were as follows: initial denaturation at 95°C for 5 m; 30 cycles of denaturation at 95°C for 30 s, annealing at 58°C for 60 s and extension at 72°C for 30 s; followed by final extension at 72°C for 10 m. PCR products were digested with BstNI (New EnglandBiolabs) at 60°C for 2 h, and were visualized using a 2% agarose gel documentation system (Bio-Rad).

2.4. Cell viability assay

Cells were seeded and grown in 96-well plates at 8×10^3 cells per well in 100μl of growth medium for 24 h based on the protocol [36]. Cells were then treated or untreated for 48 h with everolimus and sorafenib, alone or in combination. Cells were washed with phosphate buffered saline and 100 μl buffer containing 0.2 M sodium acetate (pH 5.5), 0.1% (v/v) Triton X-100 and 20 mM p-nitrophenyl phosphate was added to each of the well. The plates were incubated at 37°C for 1.5 h and the reaction was stopped by the addition of 10 μl 1M NaOH to each well and the color developed was measured at 405 nm by a microplate reader (BioRad).

2.5. Colony formation assay

Cells in single-cell suspension were plated and grown in 6-well plates at a density of 1000 cells per well for 24 h. Cells were then treated or untreated with everolimus and sorafenib, alone or combination. The medium was replaced every 3 d with fresh medium containing the corresponding agents. After 12 day treatment, the medium was removed and cell colonies were stained with 0.5% crystal violet solution.

2.6. Flow cytometric analysis and BrdU labeling

Cells were synchronized by serum starvation by growing cells in medium without serum for 2 days and then released into the cell cycle by adding 10% fetal bovine serum to the medium. The cells were untreated or treated with 10nM everolimus for 20 h, harvested, fixed with 70% ethanol, and stained with propidium iodide. The data were acquired using a flow cytometry (FACSCanto II Becton Dickinson, Franklin Lakes, NY, USA) and were analyzed using FlowJo software (Tree Star Inc., Ashland, OR, USA). BrdU pulse labeling was performed by synchronizing cells as described above. After release, the cells were exposed to BrdU (10μM) for 20 h using a FITC BrdU Flow Kit based on the manufacturers' protocol (BD Pharmingen), then fixed and permeabilized by paraformaldehyde and saponin.

After DNA was denatured using DNase, BrdU labeling was detected using a FITC conjugated antibody to BrdU.

2.7. RNA interference

For a vector-based RNA interference, double-stranded short hairpin RNA (shRNA) clones specifically targeting of *K-Ras* gene were purchased from the Mission TRC 1.0 Library (Sigma): TRCN0000010369, TRCN0000040148, TRCN0000040149, TRCN0000040152, and TRCN0000018337. MISSION vector non-target shRNA (SHC002) was used as an empty vector control. To produce shRNA lentivirus, each of the shRNA plasmids and Lentiviral Packaging Mix (Sigma, SHP001) were co-transfected into 293T cells using Fugene (Roche). After 3 day incubation, viral supernatants were isolated and passed through a 0.45-μm cellulose acetate filter. For determination of knockdown efficiency, cells were transduced and selected for 10 days in 1 μg/mL puromycin (Sigma) and the total protein were extracted for western blot. Two shRNA clones with the best knockdown efficiency were selected for further experiments.

The K-Ras knockdown PANC-1 cells were then transiently transfected either with 2 μg of p-EGFP control vector or p-EGFP/$K\text{-}Ras^{G12D}$ using Lipofectamine 2000 (Invitrogen, Carlsbad, CA). After 24 h, the efficiency of transfection was tested by fluorescent microscopy of GFP. The transfected cells were examined for the expression of $K\text{-}Ras^{G12D}$ in western blot using GFP antibody and used for experiments.

2.8. Western blot and immunoprecipitation

Cell lysates were subjected to SDS-PAGE electrophoresis and transferred to nitrocellulose membranes; the membranes were incubated overnight at 4°C with the primary antibodies, at room temperature for 1 h with HRP-conjugated secondary antibodies and developed by chemiluminescence. For immunoprecipitation, cell lysates were collected using 1% triton x-100 buffer and were incubated overnight at 4°C in a rotator with 5μl of c-Raf antibody or rabbit IgG as a negative control. Then 40 μl of protein G agarose (Invitrogen) was added and incubated with constant shaking at 4°C for another 4 hr. The beads were then gently spun down and fully washed three times with lysis buffer. Bound proteins were eluted with 2× loading buffer, then boiled and separated the protein from the beads and analyzed by western blot.

2.9. Mouse subcutaneous xenografts and treatments

The animal studies were approved by Emory University Institutional Animal Care and Use Committee. The empty vector and K-RAS shRNA expressing PANC-1 cells (7×10^6) were injected subcutaneously into the flank region of four to six-week old (about 20 g of body weight) female athymic (nu/nu) mice (Taconic, Hudson, NY). The mice were allowed to develop subcutaneous xenografts and tumor volumes were measured using calliper measurements. When tumors reached 150–200 mm^3, mice were assigned randomly to two experimental groups (n = 6/group) and treated either with saline (control) or everolimus (4 mg/kg/day, via oral gavages). Tumor volumes were measured once every 3 days and calculated based on the formula: $V = 4/3 \times \pi \times (\text{length} / 2 \times (\text{width} / 2)^2)$. After a 21-day treatment, the mice were sacrificed. The tumors were then removed and weighed. Some of the tumors were submerged in 10% neutrally buffered formalin for immunohistochemistry and others were snap-frozen in liquid nitrogen for protein extraction.

2.10. Immunohistochemistry

Five-micron thick paraffin sections were deparaffinised and rehydrated in deionized water. The sections were exposed to 3% hydrogen peroxide for 5 minutes before incubation anti-p-

ERK and p-S6 antibody at 1:50 overnight, following the approach as earlier reported [37]. The slides were then stained with secondary antibody using the R.T.U. Vectastain kit following the manufacturer's protocol (Vector Laboratories, Burlingame, CA). The slides were then exposed to 3,3'-diaminobenzidine chromogen for 5 minutes, and hematoxylin counter staining for 5 minutes.

2.11. Statistical analysis

All data were presented as means ± SE. Statistical analyses were done by using GraphPad Prism version 5.01 software programs for Windows (GraphPad Software). The difference in means between two groups were analysed with two-tailed unpaired Student's *t* –test. Results were considered to be statistically significant at $P < 0.05$.

3. Results

3.1. K-Ras mt PDAC cells are resistant to everolimus treatment

K-*Ras* mutations [33] and mTORC1 activation [37] has been shown in PDAC tissues. In exploring the correlation between K-*Ras* mutations and mTORC1 activation, we examined these in PDAC tissues surgically removed from patients. The most common K-*Ras* mutation occurs at codon 12 in PDAC tissues [33] and we confirmed this mutation in four of five PDAC tissues by PCR-RFLP analysis (Fig. 1A). In examining mTORC1 activation, we extracted total proteins from the tissues and analyzed the extracts by western blotting using antibodies against S6 and p-S6, one of the substrates of mTORC1 downstream p70S6K [3]. The expression of S6 protein was consistent in PDAC and adjacent normal pancreatic tissues tested. In contrast, western blotting revealed an increase of p-S6 protein in PDAC as compared to normal pancreatic tissues (Fig. 1B). The expression of p-S6 protein was detected in both K-*Ras* wild type (wt) and mt PDAC tissues. Immunohistochemistry further confirmed the presence of p-S6 protein in both K-*Ras* wt and mt PDAC tissues (Fig. 1C). These results demonstrate mTORC1 activation in PDAC tissues without correlation with K-*Ras* mutation in the tissues.

To examine the role of K-*Ras* mutation in PDAC resistance to rapalog, we selected PDAC cell lines that carry wt (BxPC-3, Hs776T) or mt K-*Ras* (Capan-2, PANC-1). K-*Ras* mutation in codon 12 was confirmed in Capan-2 and PANC-1 by PCR-RFLP analysis (Fig. 2A). Each of the cell lines was treated with everolimus in a series of dilutions for 48 h and cell viability assay showed that the K-*Ras* mt cell lines, Capan-2 and PANC-1, were resistant to the everolimus treatment as compared to the K-*Ras* wt BxPC-3 and Hs776T cell lines (Fig. 2B). Cell lines were then treated with 10 nM everolimus for 20 h and examined by flow cytometry to assess cell cycle (Fig. 2C). The treated cells were also examined by colony formation assay (Fig. 2D). The results showed that the everolimus treatment led to a significant increase in G1 phase in the K-*Ras* wt BxPC-3 and Hs776T but not the K-*Ras* mt Capan-2 and PANC-1 lines (Fig. 2E). Colony formation assay further revealed that the everolimus treatment significantly reduced the number of K-*Ras* wt cell lines, but not mt cell lines (Fig. 2F). The results suggest that everolimus treatment inhibits the cell cycle progression in K-*Ras* wt PDAC cells. In contrast, K-*Ras* mt PDAC cells are resistant to the treatment.

3.2. Everolimus treatment activates Ras-ERK pathway in K-Ras mt PDAC cells

To define the molecular basis of the everolimus resistance in K-*Ras* mt PDAC cells, we first examined whether everolimus treatment inhibited mTORC1 pathways in K-*Ras* mt PDAC cell lines as compared to K-*Ras* wt PDAC cell lines. Both K-*Ras* wt and mt PDAC cell lines were treated or untreated with 10 nM everolimus for 1 h. The cells were then lysed and examined by western blotting for the presence of the phosphorylated and unphosphorylated

proteins that are known to be part of the mTORC1 pathway. The everolimus treatment significantly reduced the levels of the phosphorylated proteins in mTORC1 pathway: p-mTOR, p-p70S6K and p-S6 in both the K-*Ras* wt BxPC-3 and Hs776T and K-*Ras* mt Capan-2 and PANC-1 cell lines (Fig. 3A). The results indicate that the inhibition of mTORC1 by everolimus shuts down the phosphorylation loops of mTORC1 and downstream kinases in K-*Ras* wt and mt PDAC cells. Of the two downstream kinases, S6 and 4E-BP1, the everolimus treatment inhibited S6, but not 4EBP1 in the PDAC cell lines, consistent with the reports that rapalogs differentially inhibit S6K and 4E-BP1 in the different types of cells [38; 39].

Next, we determined whether everolimus treatment activates Ras-Raf-ERK pathway in K-*Ras* mt PDAC cell lines. The everolimus treated or untreated PDAC cell lines were examined by western blotting for the presence of the phosphorylated proteins that are known to be in the Ras-Raf-ERK pathway, in which Ras interacts with c-Raf/Raf-1 and thus activates the phosphorylation loops [22]. The results showed that the everolimus treatment led to an increase in the levels of the phosphorylated proteins of Ras-Raf-ERK pathway: p-c-Raf, p-MEK, p-ERK and p-RSK in the K-*Ras* mt Capan-2 and PANC-1 but not K-*Ras* wt BxPC-3 and Hs766T cell lines (Fig. 3B), which correlates everolimus-induced Ras-Raf-ERK activation with K-*Ras* mutation in PDAC cells. To confirm this, we treated the K-*Ras* wt BxPC-3 and mt PANC-1 cell lines with everolimus in a series of dilutions for 1 h. Western blotting revealed that the everolimus treatment led to the increase of p-c-Raf, p-MEK, p-ERK and p-RSK proteins in a dose dependent manner in the K-*Ras* mt PANC-1 but not K-*Ras* wt BxPC-3 cell line (Fig. 4A). Next, we determined whether everolimus treatment enhances the interaction of mt K-Ras and c-Raf for the Ras-Raf-ERK activation. The everolimus treated and untreated K-*Ras* mt PANC-1 cells were immunoprecipitated using c-Raf antibody and western blotting using K-Ras antibody revealed the increased interaction of mt K-Ras and c-Raf protein in the everolimus treated PANC-1 cells (Fig. 4B). Taken together, these results suggest that everolimus treatment inhibits mTORC1 but activates Ras-Raf-ERK pathway in K-*Ras* mt PDAC cells.

Rapalog treatment activates PI3K/Akt pathway in human cancers and thus leads to treatment resistance [29; 40]. We sought to determine whether the rapalog-activated PI3K/Akt contributed to the rapalog resistance in K-*Ras* mt PDAC cells. The everolimus treated K-*Ras* wt and mt PDAC cell lines were examined by western blotting and the results revealed an increase in the levels of p-Akt proteins in both K-*Ras* wt and mt PDAC cell lines (Fig. 4C), suggesting that the everolimus-induced PI3K/Akt feedback loop does not contribute directly to the rapalog resistance in K-*Ras* mt PDAC cells.

3.3. Sorafenib reduces the rapalog resistance in K-Ras mt PDAC cells

Sorafenib is an multi-kinase inhibitor of c-Raf, vascular endothelial growth factor receptor-1, 2, 3 (VEGFR-1,2,3), platelet-derived growth factor receptor-β (PDGFR-β), c-kit and Flt-3 and it has been approved for clinical treatment of renal and hepatocellular carcinomas [41]. The Rasraf-ERK pathway is activated in K-*Ras* mt PDAC cells and, thus, we sought to determine whether, by inhibiting c-Raf-ERK pathway, sorafenib could release the rapalog resistance in K-*Ras* mt PDAC cells. K-*Ras* wt and mt PDAC cell lines were treated for 1 h with 10 nM everolimus and 3 μM sorafenib, alone or in combination. The sorafenib treatment inhibited the ERK pathway in both the K-*Ras* wt BxPC-3 and mt PANC-1 cell lines as evidenced by the decrease of p-MEK, p-ERK and p-RSK in the cell lines in western blot analysis (Fig 5A). In the combination with everolimus, sorafenib eliminated everolimus-induced ERK pathways in the K-Ras mt PANC-1 cells. In addition, western blotting showed that everolimus inhibited mTORC1 pathway, alone or in combination with sorafenib in the K-*Ras* mt PANC-1 cells (Fig. 5A).

The cell lines were then treated with the same doses of sorafenib and everolimus, alone or in combination, for 48 h and cell viability assay showed that the sorafenib treatment alone did not inhibit the growth of either the K-*Ras* wt BxPC-3 or K-*Ras* mt PANC-1 cells; however, in the combination, sorafenib significantly reduced the resistance of the K-*Ras* mt PANC-1 cells to the everolimus treatment (Fig. 5B). The cell lines were then treated with sorafenib and everolimus for 10 days and colony formation assay showed that the combination treatment of sorafenib and everolimus significantly reduced the size and number of the K-*Ras* mt PANC-1 cells (Fig. 5C,D). These results suggest that the combination of sorafenib and everolimus synergistically inhibits the growth of K-*Ras* mt PDAC cells through the simultaneous inhibition of mTORC1 pathway and everolimus-induced ERK pathway.

3.4. K-Ras mutation contributes to the everolimus-induced ERK signaling

Sorafenib is a multi-kinase inhibitor that inhibits c-Raf and other RTKs [41]. To specifically define the role of mt *K-Ras*, we took a knockdown approach using two K-Ras specific shRNA sequences. The shRNA sequences and empty vector as control were introduced, respectively into PDAC cell lines through lentiviral infection. Western blotting revealed the knockdown of both wt and mt K-Ras protein in the K-*Ras* wt BxPC-3 and K-*Ras* mt PANC-1 cell lines (Fig. 6A). The K-Ras shRNA expressing PDAC cell lines were treated with everolimus and cell viability assay showed that the knockdown of wt K-Ras did not affect the response of the K-Ras wt BxPC-3 cells to everolimus treatment (Fig. 6B). In contrast, however, knockdown of mt K-Ras significantly reduced the resistance of the K-*Ras* mt PANC-1 cells to everolimus (Fig. 6C). The shRNA and empty vector expressing cells were synchronized for 2 days in the FBS-free culture conditions. The cells were then released from the synchronization by adding 10% FBS in the culture medium and exposed to 10 nM everolimus and 10 μM BrdU for 20 h. Examination of the BrdU incorporation revealed that K-Ras knockdown significantly inhibited the BrdU labelling in the everolimus-treated K-*Ras* mt PANC-1 cells (Fig. 6D) but no such a effect was seen in the everolimus-treated K-Ras wt BxPC-3 cells (Fig. 6E).

Finally, K-Ras shRNA-expressing cells were treated with 10 nM everolimus for 1 h and examined by western blotting. The results showed that K-Ras knockdown significantly reduced the everolimus-induced ERK activation, as evidenced by the decrease of p-c-Raf, p-MEK and p-ERK in the K-*Ras* mt PANC-1 cell line (Fig. 6F). K-Ras shRNA knocks down both wt and mt K-*Ras* and, therefore, to confirm the role of mt *K-Ras*, the K-Ras shRNA knockdown PANC-1 cells were transfected with GFP tagged p-EGFP/K-Ras^{G12D}. The expression of mt *K-Ras*^{G12D} was confirmed by western blot using a GFP antibody, resulting in the restoration of the everolimus-induced ERK activation (Fig. 6G). Taken together, these results indicate that one mechanisms by which K-*Ras* mutation contributes to the rapalog resistance is through its activation of ERK pathway in PDAC cells. Targeting of mt K-*Ras* blocks the everolimus-induced ERK negative feedback loop and thus enhances everolimus inhibition of cell cycle progression of K-*Ras* mt PDAC cells.

3.5. IGF-1 mediates everolimus-induced EKR activation through mt K-Ras

K-Ras oncoproteins couple the RTKs of growth factors to the Raf-ERK pathway [42]. To further examine the role of mt K-Ras in this pathway, we grew K-*Ras* mt PANC-1 cell line in serum-free culture conditions supplemented with growth factors, an experimental approach that allows to examine growth factor-RKT pathway [28]. The cells grown in the serum-free culture conditions were treated or untreated first with 10 nM everolimus for 1 h and then 100 ng/ml epidermal growth factor (EGF), fibroblast growth factor 2 (FGF2), hepatocyte growth factor (HGF), IGF-1 or 10% FBS as control for 15 min. The cells were examined by western blotting and the results showed that everolimus treatment inhibited the mTORC1 pathway in the cells grown under all of these culture conditions (Fig. 7A). In

addition, everolimus treatment enhanced the ERK activation in the presence of 10% FBS and IGF-1 but not EGF, FGF2, or HGF (Fig. 7A); the results suggest that everolimus-induced ERK feedback loop occurs through IGF-1 signaling pathway.

Very recently, Ebi et al. have reported that K-Ras is an activator of the ERK pathway and RKTs are the regulators of the PI3K pathway in *K-Ras* mt colorectal carcinoma cell lines under serum culture condition [43]. To confirm the role of IGF-1, *K-Ras* mt PANC-1 cells were treated with NVP-AEW541, the IGF-1 receptor inhibitor, alone or in combination with everolimus for 8 h under our no serum culture conditions. The results showed that the treatment of NVP-AEW541 significantly reduced the IGF-1-mediated feedback activation of ERK and Akt (Fig. 7B).

To further examine the role of mt K-Ras, the experiment was repeated in the K-Ras shRNA and empty vector-expressing K-*Ras* mt PANC-1 cells. Everolimus treatment activated ERK pathway in the empty vector-expressing PNAC-1 cells in the presence of IGF-1 (Fig. 7C *left*) and stimulated the cells growth (Fig. 7D, *left*). In contrast, everolimus treatment inhibited mTORC1 without the ERK activation in the K-Ras shRNA expressing PANC-1 cells (Fig. 7C, *right*) and thus inhibited the cell growth (Fig. 7D, *right*). These results suggest that mt K-Ras is required for the everolimus-induced feedback loop of IGF-1-induced ERK pathway. Targeting of mt K-Ras eliminates the feedback loop and thus enhances the inhibitory effect of everolimus on the growth of K-Ras mt PDAC cells.

3.6. Everolimus inhibits the growth of mt K-Ras knockdown PDAC cells-derived xenografts

The *in vitro* experiments above have proved the principle that mt K-Ras contributes to the rapalog resistance through the activation of IGF-1-ERK feedback loop in K-*Ras* mt PDAC cells. To examine this *in vivo*, we generated mouse subcutaneous xenografts from the K-Ras shRNA and empty vector expressing K-*Ras* mt PANC-1 cells. Once the subcutaneous xenografts formed, mice were randomized and treated either with everolimus (4 mg/kg/day) through oral gavages in the experimental group or saline in the control group every day for twenty-one days. The size of subcutaneous xenografts were measured every three days and the results showed that everolimus treatment significantly reduced the volumes of the xenografts derived from the K-Ras shRNA expressing PANC-1 as compared with the empty vector-expressing PANC-1 cells (Fig. 8A, B).

The xenografts were removed and total protein was extracted. Western blotting confirmed the K-Ras knockdown and the inhibition of the mTORC1 pathway in the everolimus treated xenografts of the K-Ras shRNA expressing PANC-1 cells (Fig. 8C). The xenografts were also embedded in paraffin blocks and paraffin sections were examined for ERK activation using antibody to p-ERK. Immunohistochemistry confirmed the presence of p-ERK protein in the xenografts derived from the empty vector but not shRNA expressing PANC-1 cells (Fig. 8D), indicating that knockdown of mt K-Ras inhibits the ERK activation in the xenografts. In contrast, the everolimus treatment enhanced p-ERK activation in the xenografts derived from empty vector but not in shRNA expressing PANC-1 cell lines. Taken together, these results indicate that targeting of mt K-Ras can eliminate the everolimus-induced ERK feedback loop and thus enhances the therapeutic efficacy of everolimus in treating K-Ras mt PDACs through its inhibition of mTORC1 pathway.

4. Discussion

PDAC is the fourth leading cause of cancer death in the United States. Surgical resection of primary PDAC remains the only potential cure; unfortunately, however, the majority of PDACs are presented at advanced states. Current standard gemcitabine therapy and radiotherapy improve survival of patients with advanced PDAC only for up to a few months

[44; 45]. In the last decade, novel therapeutic agents have been developed targeting cancer core pathways. mTORC1 pathway is activated in human cancers [1] and thus rapalogs have been developed to target the pathway for cancer therapies [2]. The mTORC1 activation has been reported in PDAC tissues [37]; however, clinical trials have failed to show antitumor activity of rapalogs in treating PDAC patients [17; 18]. By examining K-Ras wt and mt PDAC cells in culture and xenografts, we show here that rapalog treatment activates IGF-1-mediated Ras-Raf-ERK pathway through mt K-Ras, resulting in the rapalog resistance in K-*Ras* mt PDAC cells.

Ras-ERK pathway is commonly dysregulated in PDACs and targeting of this pathway may lead to the cure of the cancers [35]. Ras activation requires the post-translational modification of its C-terminal with a farnesyl isoprenoid lipid catalyzed by farnesyl transferase (FTase) [42]. Phase II or III trials, however, have shown a limited anti-PDAC activity of tipifarnib, a FTase inhibitor [46; 47] and sorafenib, a Raf inhibitor [48; 49], alone or in combination of gemcitabine. In accordance with these clinical findings, we show here that the treatment of sorafenib alone inhibits ERK but not mTORC1 pathway and the inhibition of ERK pathway alone fails to control the growth of both K-*Ras* wt and mt PDAC cells. K-*Ras* mt PDAC cells resist everolimus treatment. However, by inhibiting the Ras-Raf-ERK feedback loop, sorafenib treatment can reduce rapalog resistance in mt K-Ras PDAC cells and thus enhance the inhibition effect of rapalog on cell growth. The study suggests that the combination of sorafenib and everolimus may provide potential therapy in treating PDAC where K-*Ras* mutation is nearly universal [35].

The results presented here show that mTORC1 pathway is activated in both K-*Ras* wt and mt PDAC tissues and cell lines. K-*Ras* wt PDAC cells respond moderately to rapalog treatment. In contrast, K-*Ras* mt PDAC cells are resistant to this treatment. These findings suggest the role of mt K-*Ras* in rapalog resistance, consistent with observations in clinical trials of rapalog treatment of human PDACs that harbour K-*Ras* mutation [17; 18] and studies of K-Ras^{G12D} engineered mouse ovarian and colonic cancers [50; 51]. Recent studies have identified two negative feedback loops in the mTORC1 signaling pathway and suggest these feedback loops may be responsible for rapalog resistance. The mTORC1 pathway is negatively regulated by mTORC1-S6K-IRS [26; 27] and mTORC1-Grb10 feedback loops [28]. By inhibiting mTORC1, rapalogs shut down these two negative feedback loops and thus activate PI3K/Akt pathway in normal and cancer cells [29; 30; 31]. Genetic ablation of mt K-*Ras* in cancer cells restores the cell response to the rapalog treatment through inhibition of rapalog-induced feedback activation of PI3K pathway [31]. In addition, prolonged rapamycin treatment seems to inhibit mTORC2 assembly and the Akt pathway [52]. These studies are therefore in accordance with the recent report that the dual PI3K and mTOR inhibitor NVP-BEZ235 inhibits the xenograft growth of primary pancreatic cancers [53].

Examination of the tumor samples from patients treated with everolimus has shown ERK activation for the first time [32]. In this study, we further show that the rapalog treatment activates ERK pathway in K-*Ras* mt PDAC cells. Knockdown of mt K-Ras blocks the rapalog-induced ERK signal, reduces the rapalog resistance, and thus enhances the therapeutic efficacy of rapalog in treating the mouse xenografts generated from K-*Ras* mt PDAC cells. IGF-1 activates mTORC1 through its RTK-mediated ERK phosphorylation and ERK-mediated inhibition of the mTORC1 inhibitors, TSC2 and RAPTOR in normal cells [22]. Recently, IGF-1 axis gene polymorphisms [54] and protein expressions [55] have been associated with the PDAC risk and aggressiveness. The results presented here further show that rapalog-induced ERK activation occurs through the IGF-1 signaling pathway and mt K-Ras is required for the rapalog-induced IGF-1-ERK activation and thus contributes to the rapalog resistance in K-*Ras* mt PDAC.

In conclusion, the findings presented here provide the rationale for a combination of K-Ras and mTORC1 inhibitors in the treatment of PDAC where K-*Ras* mutations are nearly universal. K-Ras mutations contribute to rapalog-induced feedback activation of IGF-1-ERK pathway and thus targeting of mt K-Ras blocks the feedback ERK signal, reduced rapalog resistance and thus enhances therapeutic efficacy of rapalogs in treating human PDAC. New cancer therapeutic agents are indeed currently under development for the combination therapies that simultaneously target the multiple core pathways in cancers [8].

Acknowledgments

Funding NIH/NCI R01 grant CA129687 (C.H.), NIH/NCI R01 grant CA118450 (S.Y.S.).

References

[1]. Zoncu R, Efeyan A, Sabatini DM. mTOR: from growth signal integration to cancer, diabetes and ageing. Nat Rev Mol Cell Biol. 2011; 12:21–35. [PubMed: 21157483]

[2]. Faivre S, Kroemer G, Raymond E. Current development of mTOR inhibitors as anticancer agents. Nat Rev Drug Discov. 2006; 5:671–688. [PubMed: 16883305]

[3]. Ma XM, Blenis J. Molecular mechanisms of mTOR-mediated translational control. Nat Rev Mol Cell Biol. 2009; 10:307–318. [PubMed: 19339977]

[4]. Kim DH, Sarbassov DD, Ali SM, King JE, Latek RR, Erdjument-Bromage H, Tempst P, Sabatini DM. mTOR interacts with raptor to form a nutrient-sensitive complex that signals to the cell growth machinery. Cell. 2002; 110:163–175. [PubMed: 12150925]

[5]. Loewith R, Jacinto E, Wullschleger S, Lorberg A, Crespo JL, Bonenfant D, Oppliger W, Jenoe P, Hall MN. Two TOR complexes, only one of which is rapamycin sensitive, have distinct roles in cell growth control. Mol Cell. 2002; 10:457–468. [PubMed: 12408816]

[6]. Guertin DA, Sabatini DM. Defining the role of mTOR in cancer. Cancer Cell. 2007; 12:9–22. [PubMed: 17613433]

[7]. Meric-Bernstam F, Gonzalez-Angulo AM. Targeting the mTOR signaling network for cancer therapy. J Clin Oncol. 2009; 27:2278–2287. [PubMed: 19332717]

[8]. Wander SA, Hennessy BT, Slingerland JM. Next-generation mTOR inhibitors in clinical oncology: how pathway complexity informs therapeutic strategy. J Clin Invest. 2011; 121:1231–1241. [PubMed: 21490404]

[9]. Hudes G, Carducci M, Tomczak P, Dutcher J, Figlin R, Kapoor A, Staroslawska E, Sosman J, McDermott D, Bodrogi I, Kovacevic Z, Lesovoy V, Schmidt-Wolf IG, Barbarash O, Gokmen E, O'Toole T, Lustgarten S, Moore L, Motzer RJ. Temsirolimus, interferon alfa, or both for advanced renal-cell carcinoma. N Engl J Med. 2007; 356:2271–2281. [PubMed: 17538086]

[10]. Motzer RJ, Escudier B, Oudard S, Hutson TE, Porta C, Bracarda S, Grunwald V, Thompson JA, Figlin RA, Hollaender N, Urbanowitz G, Berg WJ, Kay A, Lebwohl D, Ravaud A. Efficacy of everolimus in advanced renal cell carcinoma: a double-blind, randomised, placebo-controlled phase III trial. Lancet. 2008; 372:449–456. [PubMed: 18653228]

[11]. Hess G, Herbrecht R, Romaguera J, Verhoef G, Crump M, Gisselbrecht C, Laurell A, Offner F, Strahs A, Berkenblit A, Hanushevsky O, Clancy J, Hewes B, Moore L, Coiffier B. Phase III study to evaluate temsirolimus compared with investigator's choice therapy for the treatment of relapsed or refractory mantle cell lymphoma. J Clin Oncol. 2009; 27:3822–3829. [PubMed: 19581539]

[12]. Yao JC, Shah MH, Ito T, Bohas CL, Wolin EM, Van Cutsem E, Hobday TJ, Okusaka T, Capdevila J, de Vries EG, Tomassetti P, Pavel ME, Hoosen S, Haas T, Lincy J, Lebwohl D, Oberg K. Everolimus for advanced pancreatic neuroendocrine tumors. N Engl J Med. 2011; 364:514–523. [PubMed: 21306238]

[13]. Galanis E, Buckner JC, Maurer MJ, Kreisberg JI, Ballman K, Boni J, Peralba JM, Jenkins RB, Dakhil SR, Morton RF, Jaeckle KA, Scheithauer BW, Dancey J, Hidalgo M, Walsh DJ. Phase II trial of temsirolimus (CCI-779) in recurrent glioblastoma multiforme: a North Central Cancer Treatment Group Study. J Clin Oncol. 2005; 23:5294–5304. [PubMed: 15998902]

[14]. Margolin K, Longmate J, Baratta T, Synold T, Christensen S, Weber J, Gajewski T, Quirt I, Doroshow JH. CCI-779 in metastatic melanoma: a phase II trial of the California Cancer Consortium. Cancer. 2005; 104:1045–1048. [PubMed: 16007689]

[15]. Chan S, Scheulen ME, Johnston S, Mross K, Cardoso F, Dittrich C, Eiermann W, Hess D, Morant R, Semiglazov V, Borner M, Salzberg M, Ostapenko V, Illiger HJ, Behringer D, Bardy-Bouxin N, Boni J, Kong S, Cincotta M, Moore L. Phase II study of temsirolimus (CCI-779), a novel inhibitor of mTOR, in heavily pretreated patients with locally advanced or metastatic breast cancer. J Clin Oncol. 2005; 23:5314–5322. [PubMed: 15955899]

[16]. Ellard SL, Clemons M, Gelmon KA, Norris B, Kennecke H, Chia S, Pritchard K, Eisen A, Vandenberg T, Taylor M, Sauerbrei E, Mishaeli M, Huntsman D, Walsh W, Olivo M, McIntosh L, Seymour L. Randomized phase II study comparing two schedules of everolimus in patients with recurrent/metastatic breast cancer: NCIC Clinical Trials Group IND.163. J Clin Oncol. 2009; 27:4536–4541. [PubMed: 19687332]

[17]. Wolpin BM, Hezel AF, Abrams T, Blaszkowsky LS, Meyerhardt JA, Chan JA, Enzinger PC, Allen B, Clark JW, Ryan DP, Fuchs CS. Oral mTOR inhibitor everolimus in patients with gemcitabine-refractory metastatic pancreatic cancer. J Clin Oncol. 2009; 27:193–198. [PubMed: 19047305]

[18]. Javle MM, Shroff RT, Xiong H, Varadhachary GA, Fogelman D, Reddy SA, Davis D, Zhang Y, Wolff RA, Abbruzzese JL. Inhibition of the mammalian target of rapamycin (mTOR) in advanced pancreatic cancer: results of two phase II studies. BMC Cancer. 2010; 10:368. [PubMed: 20630061]

[19]. Sengupta S, Peterson TR, Sabatini DM. Regulation of the mTOR complex 1 pathway by nutrients, growth factors, and stress. Mol Cell. 2010; 40:310–322. [PubMed: 20965424]

[20]. Inoki K, Li Y, Zhu T, Wu J, Guan KL. TSC2 is phosphorylated and inhibited by Akt and suppresses mTOR signalling. Nat Cell Biol. 2002; 4:648–657. [PubMed: 12172553]

[21]. Vander Haar E, Lee SI, Bandhakavi S, Griffin TJ, Kim DH. Insulin signalling to mTOR mediated by the Akt/PKB substrate PRAS40. Nat Cell Biol. 2007; 9:316–323. [PubMed: 17277771]

[22]. Mendoza MC, Er EE, Blenis J. The Ras-ERK and PI3K-mTOR pathways: cross-talk and compensation. Trends Biochem Sci. 2011; 36:320–328. [PubMed: 21531565]

[23]. Ballif BA, Roux PP, Gerber SA, MacKeigan JP, Blenis J, Gygi SP. Quantitative phosphorylation profiling of the ERK/p90 ribosomal S6 kinase-signaling cassette and its targets, the tuberous sclerosis tumor suppressors. Proc Natl Acad Sci U S A. 2005; 102:667–672. [PubMed: 15647351]

[24]. Ma L, Chen Z, Erdjument-Bromage H, Tempst P, Pandolfi PP. Phosphorylation and functional inactivation of TSC2 by Erk implications for tuberous sclerosis and cancer pathogenesis. Cell. 2005; 121:179–193. [PubMed: 15851026]

[25]. Carriere A, Romeo Y, Acosta-Jaquez HA, Moreau J, Bonneil E, Thibault P, Fingar DC, Roux PP. ERK1/2 phosphorylate Raptor to promote Ras-dependent activation of mTOR complex 1 (mTORC1). J Biol Chem. 2011; 286:567–577. [PubMed: 21071439]

[26]. Shah OJ, Wang Z, Hunter T. Inappropriate activation of the TSC/Rheb/mTOR/S6K cassette induces IRS1/2 depletion, insulin resistance, and cell survival deficiencies. Curr Biol. 2004; 14:1650–1656. [PubMed: 15380067]

[27]. Tzatsos A, Kandror KV. Nutrients suppress phosphatidylinositol 3-kinase/Akt signaling via raptor-dependent mTOR-mediated insulin receptor substrate 1 phosphorylation. Mol Cell Biol. 2006; 26:63–76. [PubMed: 16354680]

[28]. Yu Y, Yoon SO, Poulogiannis G, Yang Q, Ma XM, Villen J, Kubica N, Hoffman GR, Cantley LC, Gygi SP, Blenis J. Phosphoproteomic analysis identifies Grb10 as an mTORC1 substrate that negatively regulates insulin signaling. Science. 2011; 332:1322–1326. [PubMed: 21659605]

[29]. O'Reilly KE, Rojo F, She QB, Solit D, Mills GB, Smith D, Lane H, Hofmann F, Hicklin DJ, Ludwig DL, Baselga J, Rosen N. mTOR inhibition induces upstream receptor tyrosine kinase signaling and activates Akt. Cancer Res. 2006; 66:1500–1508. [PubMed: 16452206]

[30]. Wang X, Yue P, Kim YA, Fu H, Khuri FR, Sun SY. Enhancing mammalian target of rapamycin (mTOR)-targeted cancer therapy by preventing mTOR/raptor inhibition-initiated, mTOR/rictor-independent Akt activation. Cancer Res. 2008; 68:7409–7418. [PubMed: 18794129]

[31]. Di Nicolantonio F, Arena S, Tabernero J, Grosso S, Molinari F, Macarulla T, Russo M, Cancelliere C, Zecchin D, Mazzucchelli L, Sasazuki T, Shirasawa S, Geuna M, Frattini M, Baselga J, Gallicchio M, Biffo S, Bardelli A. Deregulation of the PI3K and KRAS signaling pathways in human cancer cells determines their response to everolimus. J Clin Invest. 2010; 120:2858–2866. [PubMed: 20664172]

[32]. Carracedo A, Ma L, Teruya-Feldstein J, Rojo F, Salmena L, Alimonti A, Egia A, Sasaki AT, Thomas G, Kozma SC, Papa A, Nardella C, Cantley LC, Baselga J, Pandolfi PP. Inhibition of mTORC1 leads to MAPK pathway activation through a PI3K-dependent feedback loop in human cancer. J Clin Invest. 2008; 118:3065–3074. [PubMed: 18725988]

[33]. Almoguera C, Shibata D, Forrester K, Martin J, Arnheim N, Perucho M. Most human carcinomas of the exocrine pancreas contain mutant c-K-ras genes. Cell. 1988; 53:549–554. [PubMed: 2453289]

[34]. Scheffzek K, Ahmadian MR, Kabsch W, Wiesmuller L, Lautwein A, Schmitz F, Wittinghofer A. The Ras-RasGAP complex: structural basis for GTPase activation and its loss in oncogenic Ras mutants. Science. 1997; 277:333–338. [PubMed: 9219684]

[35]. Morris, J.P.t.; Wang, SC.; Hebrok, M. KRAS, Hedgehog, Wnt and the twisted developmental biology of pancreatic ductal adenocarcinoma. Nat Rev Cancer. 2010; 10:683–695. [PubMed: 20814421]

[36]. Bellail AC, Tse MC, Song JH, Phuphanich S, Olson JJ, Sun SY, Hao C. DR5-mediated DISC controls caspase-8 cleavage and initiation of apoptosis in human glioblastomas. J Cell Mol Med. 2010; 14:1303–1317. [PubMed: 19432816]

[37]. Bellizzi AM, Bloomston M, Zhou XP, Iwenofu OH, Frankel WL. The mTOR pathway is frequently activated in pancreatic ductal adenocarcinoma and chronic pancreatitis. Appl Immunohistochem Mol Morphol. 2010; 18:442–447. [PubMed: 20661135]

[38]. Choo AY, Yoon SO, Kim SG, Roux PP, Blenis J. Rapamycin differentially inhibits S6Ks and 4E-BP1 to mediate cell-type-specific repression of mRNA translation. Proc Natl Acad Sci U S A. 2008; 105:17414–17419. [PubMed: 18955708]

[39]. Yu K, Toral-Barza L, Shi C, Zhang WG, Lucas J, Shor B, Kim J, Verheijen J, Curran K, Malwitz DJ, Cole DC, Ellingboe J, Ayral-Kaloustian S, Mansour TS, Gibbons JJ, Abraham RT, Nowak P, Zask A. Biochemical, cellular, and in vivo activity of novel ATP-competitive and selective inhibitors of the mammalian target of rapamycin. Cancer Res. 2009; 69:6232–6240. [PubMed: 19584280]

[40]. Sun SY, Rosenberg LM, Wang X, Zhou Z, Yue P, Fu H, Khuri FR. Activation of Akt and eIF4E survival pathways by rapamycin-mediated mammalian target of rapamycin inhibition. Cancer Res. 2005; 65:7052–7058. [PubMed: 16103051]

[41]. Iyer R, Fetterly G, Lugade A, Thanavala Y. Sorafenib: a clinical and pharmacologic review. Expert Opin Pharmacother. 2010; 11:1943–1955. [PubMed: 20586710]

[42]. Karnoub AE, Weinberg RA. Ras oncogenes: split personalities. Nat Rev Mol Cell Biol. 2008; 9:517–531. [PubMed: 18568040]

[43]. Ebi H, Corcoran RB, Singh A, Chen Z, Song Y, Lifshits E, Ryan DP, Meyerhardt JA, Benes C, Settleman J, Wong KK, Cantley LC, Engelman JA. Receptor tyrosine kinases exert dominant control over PI3K signaling in human KRAS mutant colorectal cancers. J Clin Invest. 2011; 121:4311–4321. [PubMed: 21985784]

[44]. Mulcahy MF, Wahl AO, Small W Jr. The current status of combined radiotherapy and chemotherapy for locally advanced or resected pancreas cancer. J Natl Compr Canc Netw. 2005; 3:637–642. [PubMed: 16194455]

[45]. Gutt R, Liauw SL, Weichselbaum RR. The role of radiotherapy in locally advanced pancreatic carcinoma. Nat Rev Gastroenterol Hepatol. 2010; 7:437–447. [PubMed: 20628346]

[46]. Cohen SJ, Ho L, Ranganathan S, Abbruzzese JL, Alpaugh RK, Beard M, Lewis NL, McLaughlin S, Rogatko A, Perez-Ruixo JJ, Thistle AM, Verhaeghe T, Wang H, Weiner LM, Wright JJ, Hudes GR, Meropol NJ. Phase II and pharmacodynamic study of the farnesyltransferase inhibitor R115777 as initial therapy in patients with metastatic pancreatic adenocarcinoma. J Clin Oncol. 2003; 21:1301–1306. [PubMed: 12663718]

[47]. Van Cutsem E, van de Velde H, Karasek P, Oettle H, Vervenne WL, Szawlowski A, Schoffski P, Post S, Verslype C, Neumann H, Safran H, Humblet Y, Perez Ruixo J, Ma Y, Von Hoff D. Phase III trial of gemcitabine plus tipifarnib compared with gemcitabine plus placebo in advanced pancreatic cancer. J Clin Oncol. 2004; 22:1430–1438. [PubMed: 15084616]

[48]. Kindler HL, Wroblewski K, Wallace JA, Hall MJ, Locker G, Nattam S, Agamah E, Stadler WM, Vokes EE. Gemcitabine plus sorafenib in patients with advanced pancreatic cancer: a phase II trial of the University of Chicago Phase II Consortium. Invest New Drugs. 2010

[49]. El-Khoueiry AB, Ramanathan RK, Yang DY, Zhang W, Shibata S, Wright JJ, Gandara D, Lenz HJ. A randomized phase II of gemcitabine and sorafenib versus sorafenib alone in patients with metastatic pancreatic cancer. Invest New Drugs. 2011

[50]. Hung KE, Maricevich MA, Richard LG, Chen WY, Richardson MP, Kunin A, Bronson RT, Mahmood U, Kucherlapati R. Development of a mouse model for sporadic and metastatic colon tumors and its use in assessing drug treatment. Proc Natl Acad Sci U S A. 2010; 107:1565–1570. [PubMed: 20080688]

[51]. Xing D, Orsulic S. A genetically defined mouse ovarian carcinoma model for the molecular characterization of pathway-targeted therapy and tumor resistance. Proc Natl Acad Sci U S A. 2005; 102:6936–6941. [PubMed: 15860581]

[52]. Sarbassov DD, Ali SM, Sengupta S, Sheen JH, Hsu PP, Bagley AF, Markhard AL, Sabatini DM. Prolonged rapamycin treatment inhibits mTORC2 assembly and Akt/PKB. Mol Cell. 2006; 22:159–168. [PubMed: 16603397]

[53]. Cao P, Maira SM, Garcia-Echeverria C, Hedley DW. Activity of a novel, dual PI3-kinase/mTor inhibitor NVP-BEZ235 against primary human pancreatic cancers grown as orthotopic xenografts. Br J Cancer. 2009; 100:1267–1276. [PubMed: 19319133]

[54]. Dong X, Li Y, Tang H, Chang P, Hess KR, Abbruzzese JL, Li D. Insulin-like growth factor axis gene polymorphisms modify risk of pancreatic cancer. Cancer Epidemiol. 2011

[55]. Kwon J, Stephan S, Mukhopadhyay A, Muders MH, Dutta SK, Lau JS, Mukhopadhyay D. Insulin receptor substrate-2 mediated insulin-like growth factor-I receptor overexpression in pancreatic adenocarcinoma through protein kinase Cdelta. Cancer Res. 2009; 69:1350–1357. [PubMed: 19190347]

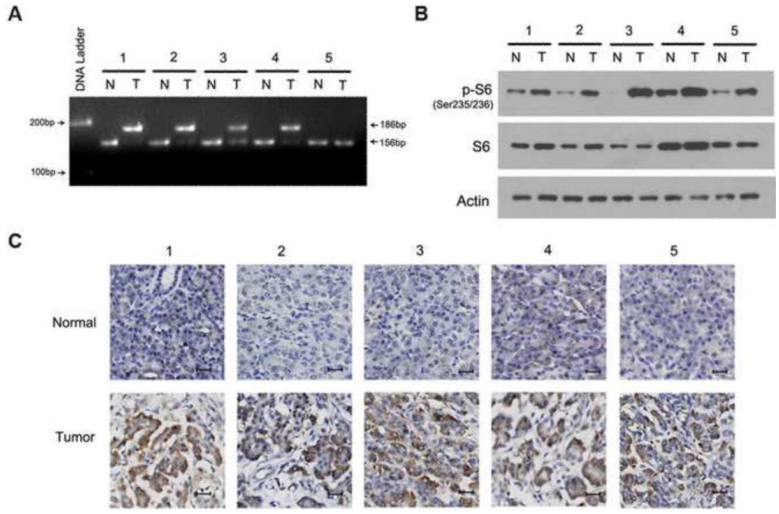

Fig. 1.

The activation of mTORC1 in PDAC tissues. (A) PCR-RFLP analysis of K-*Ras* mt (186-bp DNA fragment) and wt (156-bp DNA fragment) in five PDAC tumors (T) and matched adjacent normal pancreatic tissues (N). (B) Western blot analysis of S6 and p-S6 protein in PDAC tumors (T) and normal pancreatic tissues (N). Actin was used as a loading control. (C) IHC examination of p-S6 protein in the K-*Ras* wt and mt PDAC tumors and matched normal pancreatic tissues (bar, 20 μM).

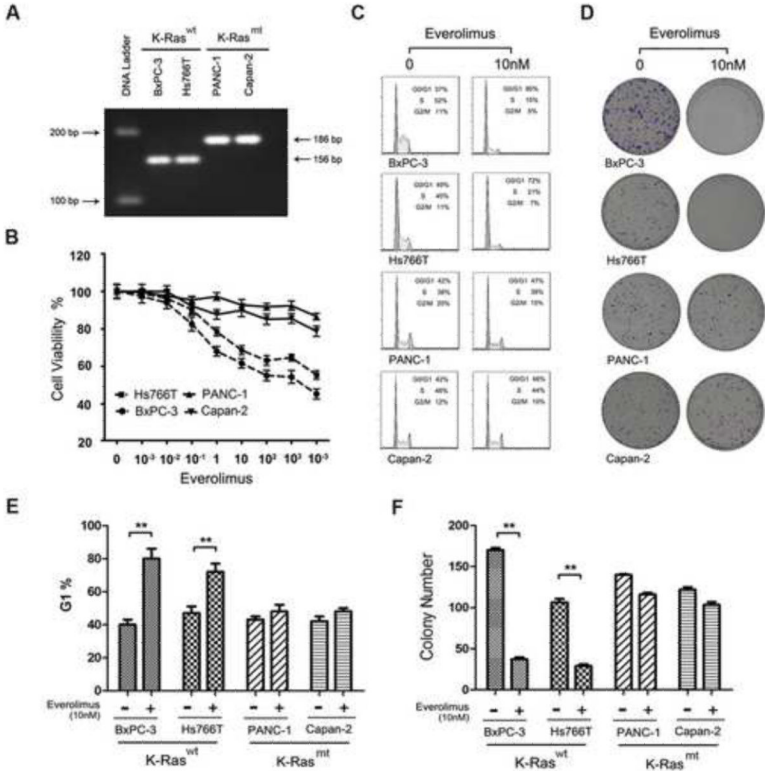

Fig. 2.

K-*Ras* mutations in PDAC correlate to rapalog resistance. (A) PCR-RFLP analysis of K-*Ras* mt and wt in four PDAC cell lines, BxPC-3, Hs766T, PANC-1 and Capan-2. (B) Cell viability assay of the response of the K-*Ras* wt Hs766T and BxPC-3 and K-*Ras* mt PANC-1 and Capan-2 cell lines to everolimus treatment. (C) Flow cytometry cell cycle analysis of PDAC cell lines untreated (0nM) or treated with 10nM everolimus. The cells in G/G1, S and G2/M phase were presented in the percentage. (D) Colony formation assay of PDAC cell lines treated or untreated with everolimus, showing the colony densities in the culture wells. (E) The data from flow cytometry as presented in C above were statistically analyzed. The experiment was repeated three times and the percentage of G1 cells was presented as mean ± SD. **, $p < 0.01$. F. The colony formation data as presented in D above were statistically analyzed. The experiment was repeated three times and the number of colonies was presented as mean ± SD. **, $p < 0.01$.

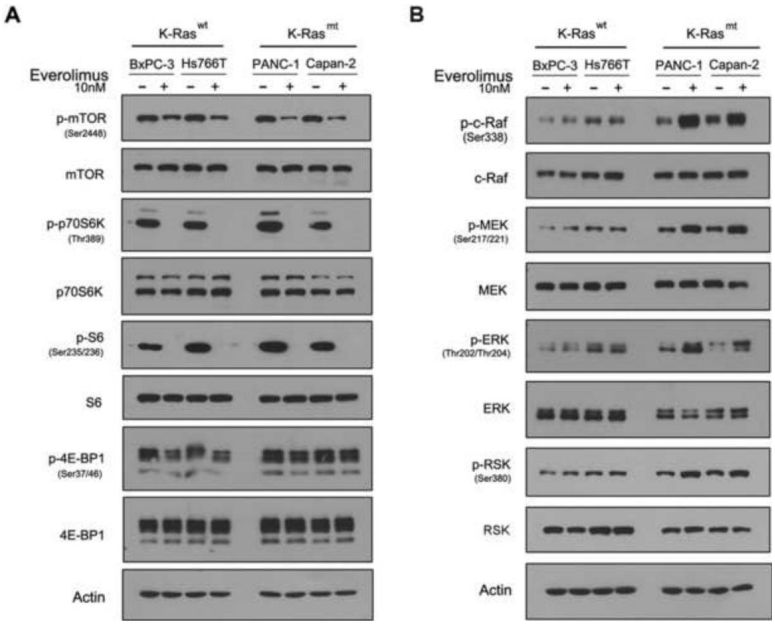

Fig. 3.

Everolimus inhibits mTORC1 but activates ERK pathway in K-*Ras* mt PDAC cells. Everolimus treated or untreated K-*Ras* wt and mt PDAC cell lines, as indicated on the top of the panel, were examined by western blotting using antibodies to the unphosphorylated and phosphorylated (p-) proteins in the mTORC1 (A) and Raf-ERK pathway (B), as indicated to the left of the panel.

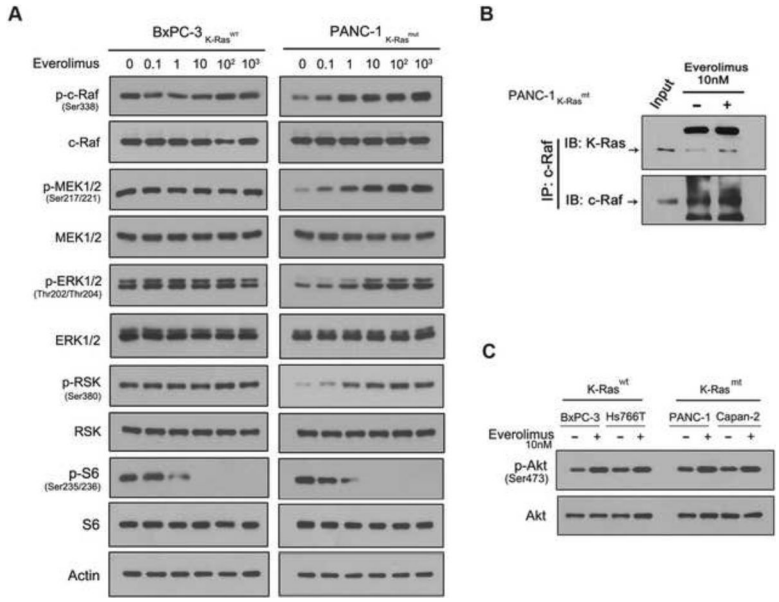

Fig. 4.

Everolimus treatment enhances the interaction of K-Ras and c-Raf. (A) The K-*Ras* wt BxPC-3 and K-*Ras* mt PANC-1 were treated with everolimus in a series of dilutions and examined by western blotting for the unphosphorylated and phosphorylated (p-) proteins in the Raf-ERK and mTORC1 pathways. (B) The everolimus treated and untreated K-*Ras* mt PANC-1 cells were immunoprecipitated using c-Raf antibody and then examined by western blotting using K-Ras and c-Raf antibody for the interaction of K-Ras and c-Raf proteins. (C) The K-Ras wt BxPC-3 and Hs766T and K-Ras mt PANC-1 and Capan-2 cell lines were treated with everolimus and examined by western blotting using p-Akt and Akt antibodies.

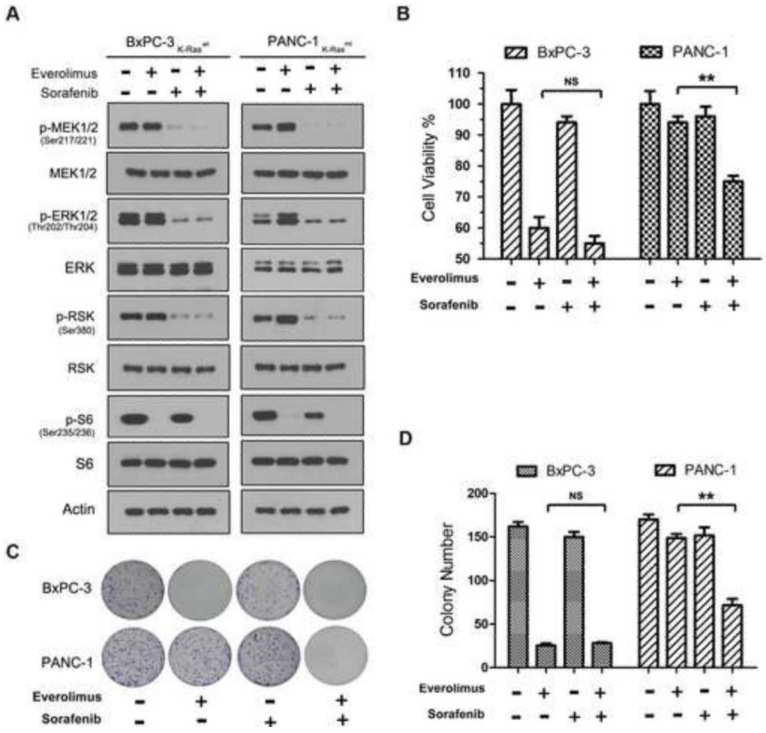

Fig. 5.

Sorafenib reduces rapalog resistance through inhibition of Raf-ERK pathway. (A) The K-*Ra*s wt BxPC3 and K-*Ra*s mt PANC-1 cell lines were treated with everolimus and sorafenib, alone or in combination, as indicated on the top of the panel, and then examined by western blotting using antibodies to the unphosphorylated and phosphorylated (p-) proteins in the Raf-ERK and mTORC1 pathway. (B) The K-*Ra*s wt BxPC-3 and mt PANC-1 were treated with everolimus and sorafenib, alone or in combination, and examined by cell viability assay (NS, not significant; **, $p < 0.01$). (C) The treated or untreated cells as described above were further examined by colony formation assay. (D) The experiment was repeated three times and statistically analyzed. The number of colonies was presented as mean ± SD (NS, not significant; **, $p < 0.01$).

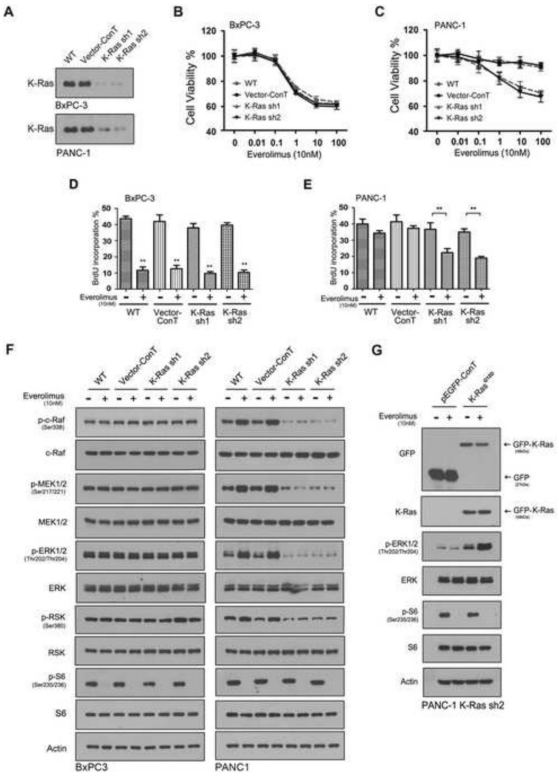

Fig. 6.

Knockdown of mt K-*Ras* reduces rapalog resistance through eliminating everolimus-induced ERK loop. (A) BxPC-3 and PANC-1 cell lines (WT) were introduced with empty-vector as control (vector-ConT) and K-*Ras* shRNA sequence 1 (sh1) and 2 (sh2) and examined by western blotting using K-*Ras* antibody for the K-Ras knockdown. (B & C) The empty vector and K-*Ras* shRNA expressing BxPC-3 (B) and PANC-1 cells (C) were treated with everolimus and examined by cell viability assay. (D & E) The vector and K-*Ras* shRNA expressing BxPC-3 (D) and PANC-1 cells (E) were treated with everolimus and examined by BrdU labeling. The BrdU incorporated cells were presented in the percentage. The experiment was repeated three times and the data was presented as mean ± SD. **, $p < 0.01$. (F) The vector and K-*Ras* shRNA expressing BxPC-3 and PANC-1 cells were treated with everolimus and examined by western blotting using antibodies to the phosphorylated and unphosphorylated proteins in the Raf-ERK and mTORC1 pathways. (G) PANC-1 K-Ras knockdown cells were transfected with p-EGFP vector or p-EGFP/K-Ras^{G12D}, treated with 10nM Everolimus for 1h and subjected to western blot analysis. The GFP-K-Ras^{G12D} protein was indicated to the right side of the panel.

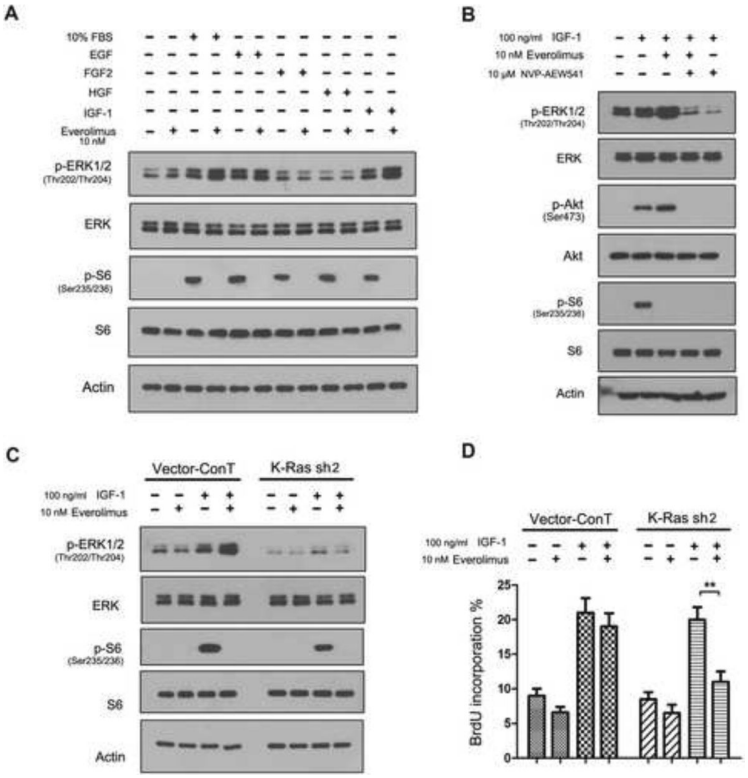

Figure 7.

K-*Ras* mutations contribute to the everolimus-induced ERK signal. (A) The K-*Ras* mt PANC-1 cells were subjected to western blotting after treated first with everolimus and then exposed to 10% FBS, EGF, FGF2, HGF and IGF-1, as indicated on the top of the panel. (B) The experiment was repeated with using NVP-AEW541. (C) The empty vector and K-*Ras* shRNA expressing PANC-1 cells were examined by western blotting after treated first with everolimus first and then with IGF-1. (D) The empty vector and K-*Ras* shRNA expressing PANC-1 cells, treated as described above in B, were examined by by BrdU labeling assay. The experiment was repeated three times and the data was presented as mean ± SD. **, $p < 0.01$.

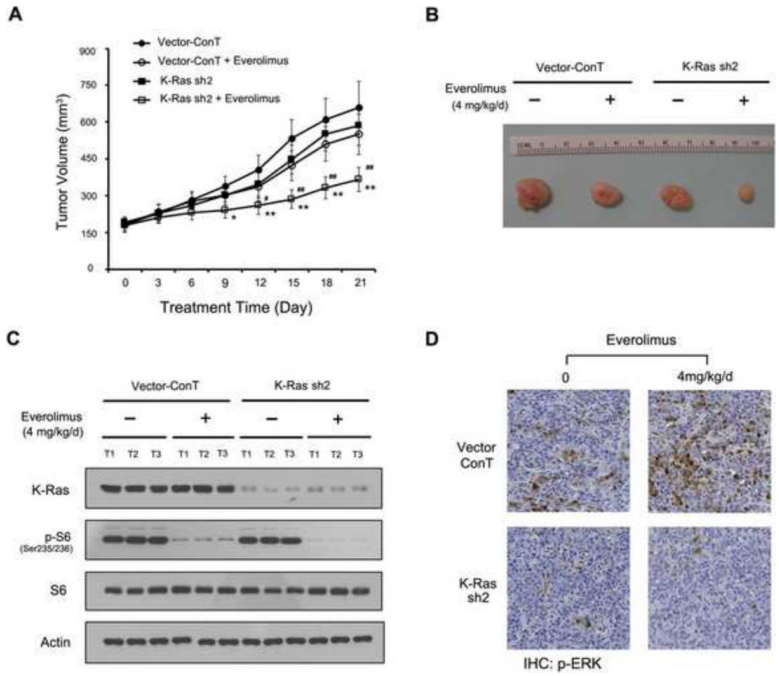

Figure 8.

K-*Ras* knockdown enhances the therapeutic efficacy of everolimus in treating PDAC xenografts. (A) Mouse subcutaneous PDAC xenografts were generated from empty vector and K-Ras shRNA sequence 2 (sh2) and treated either with everolimus (4 mg/kg/day) in the experimental group or saline in the control group for the days as indicated. The tumor volumes from the same group mice were presented as mean±SD and statistically analysed. *, $p < 0.05$ and **, $p < 0.01$ as compared with control and #, $p < 0.05$ and ##, $p < 0.01$ as compared with everolimus treatment. (B) The representative xenografts were shown from the experimental and control group. (C) The vector or K-Ras shRNA cells-derived xenografts, treated or untreated with everolimus, were examined by western blotting using antibodies to K-Ras, p-S6, S6 and actin as a loading control. (D) The xenografts were also embedded in paraffin blocks and paraffin sections were examined by immunohistochemistry using p-ERK antibody.